

Melanie Aldridge¹, Chirag Patel²,
Andrew Mallett^{3,4} and Peter Trnka^{1,4}

¹Department of Nephrology, Lady Cilento Children's Hospital, South Brisbane, Queensland, Australia; ²Genetic Health Queensland, Royal Brisbane and Women's Hospital, Herston, Queensland, Australia; ³Kidney Health Service and Conjoint Renal Research Laboratory, Royal Brisbane and Women's Hospital, Herston, Queensland, Australia; and ⁴Faculty of Medicine, The University of Queensland, Herston, Queensland, Australia
Corresponding author: Melanie Aldridge, Child & Adolescent Renal Service, Lady Cilento Children's Hospital, 501 Stanley Street, South Brisbane, Queensland, Australia. E-mail: melanie.aldrige@health.qld.gov.au

DISCLOSURE

AM has been a member of the tolvaptan Medical Advisory Board for Otsuka Australia Pharmaceutical Pty Ltd. All the other authors declared no competing interests.

SUPPLEMENTARY MATERIAL

Supplementary Methods.

Supplementary material is linked to the online version of the paper at www.kireports.org.

REFERENCES

- Boyer O, Gagnadoux M, Guest G, et al. Prognosis of autosomal dominant polycystic kidney disease diagnosed in utero or at birth. *Pediatr Nephrol.* 2007;22:380–388.
- Sweeney W, Avner E. Diagnosis and management of childhood polycystic kidney disease. *Pediatr Nephrol.* 2011;26:675–692.
- Mekahli D, Woolf A, Bockenbauer D. Similar renal outcomes in children with ADPKD diagnosed by screening or presenting with symptoms. *Pediatr Nephrol.* 2010;22:2275–2282.
- Rangan G, Alexander S, Campbell K. KHA-CARI guideline recommendations for the diagnosis and management of autosomal dominant polycystic kidney disease. *Nephrology.* 2016;21:705–716.
- Rizk D, Chapman A. Treatment of autosomal dominant polycystic kidney disease (ADPKD): the new horizon for children with ADPKD. *Pediatr Nephrol.* 2008;23:1029–1036.
- Helal I, Reed B, McFann K, et al. Glomerular hyperfiltration and renal progression in children with autosomal dominant polycystic kidney disease. *Clin J Am Soc Nephrol.* 2011;6:2439–2443.
- Fencil F, Janda J, Blahova K, et al. Genotype-phenotype correlation in children with autosomal dominant polycystic kidney disease. *Pediatr Nephrol.* 2009;24:983–989.
- Cornec-Le Gall E, Audrezet MA, Rousseau A, et al. The PROPKD score: a new algorithm to predict renal survival in autosomal dominant polycystic kidney disease. *J Am Soc Nephrol.* 2015;27:942–951.
- Fick-Brosnahan G, Tran Z, Johnson A, et al. Progression of autosomal-dominant polycystic kidney disease in children. *Kidney Int.* 2001;59:1654–1662.
- Mai J, Lee V, Lopez-Vargas P, Vladica P. KHA-CARI autosomal dominant polycystic kidney disease guideline: imaging approaches for diagnosis. *Semin Nephrol.* 2015;35:538–544.
- De Rechter S, Kringen J, Janssens P, et al. Clinician's attitude towards family planning and timing of diagnosis in autosomal dominant polycystic kidney disease. *PLoS One.* 2017;12:e0185779.
- Patel C, Tchan M, Savige J, et al. KHA-CARI autosomal dominant polycystic kidney disease guideline: genetics and genetic counselling. *Semin Nephrol.* 2015;35:550–556.
- Tan YC, Blumenfeld J, Rennert H. Autosomal dominant polycystic kidney disease: genetics, mutations and micro-RNAs. *Biochim Biophys Acta.* 2011;1812:1202–1212.
- Tchan M, Savig J, Patel C, et al. KHA-CARI autosomal dominant polycystic kidney disease guideline: genetic testing for diagnosis. *Semin Nephrol.* 2015;35:545–549.
- Antignac C, Calvet JP, Cermino GG, et al. The future of polycystic kidney disease research—as seen by the 12 Kaplan Awardees. *J Am Soc Nephrol.* 2015;26:2081–2095.
- Queensland Government. Queensland population counter. Available at: <http://www.qgso.qld.gov.au/products/reports/pop-growth-qld/qld-pop-counter.php>. Accessed February 14, 2018.
- Gimpel C, Avni F, Bergmann C, et al. Perinatal diagnosis, management, and follow up of cystic renal diseases: a clinical practice recommendation with systematic literature reviews. *JAMA.* 2018;172:74–86.
- US National Library of Medicine. Safety pharmacokinetics, tolerability and efficacy of tolvaptan in children and adolescents with ADPKD (autosomal dominant polycystic kidney disease). Available at: <https://clinicaltrials.gov/ct2/show/NCT02964273>. Accessed January 2, 2018.
- Polycystic Kidney Disease Foundation. ADPKD Mutation Database. Available at: <http://pkdb.pkdcure.org>. Accessed October 28, 2017.
- Cornec-Le Gall E, Audrezet MP, Chen JM, et al. Type of PKD1 mutation influences renal outcome in ADPKD. *J Am Soc Nephrol.* 2013;24:1006–1013.

Received 8 March 2018; revised 19 April 2018; accepted 7 May 2018; published online 15 May 2018

Kidney Int Rep (2018) 3, 1217; <https://doi.org/10.1016/j.kir.2018.05.002>

Crown Copyright © 2018 Published by Elsevier Inc. on behalf of International Society of Nephrology. This is an open access article under the CC BY-NC-ND license (<http://creativecommons.org/licenses/by-nc-nd/4.0/>).

The Role of Oxidative Stress and Inflammation in Acute Oxalate Nephropathy Associated With Ethylene Glycol Intoxication



To the Editor: Calcium oxalate crystal (CaOx) deposition within the renal parenchyma is well described as

a cause of both acute kidney injury and chronic kidney disease. Animal and cell line studies have previously demonstrated that this injury is modulated by oxidative stress—induced danger-associated molecular patterns following CaOx deposition within the interstitium^{1,2}. It has been postulated that these oxidative stress-induced danger-associated molecular patterns may participate in the pathogenesis of acute kidney injury and chronic kidney disease in humans, leading to the recruitment of an inflammatory response characterized by an increased infiltration of monocytes and macrophages.^{1,3,4} However, evidence of this mechanism in humans is lacking. We report the morphological changes in renal cortical tissue from a 36-year-old woman with acute oxalate nephropathy secondary to ethylene glycol intoxication, and correlate them with a marker of oxidative stress and cell populations in an associated inflammatory infiltrate. Our findings provide initial evidence linking renal deposits of CaOx to oxidative stress and inflammation in humans.

A 36-year-old woman was brought to hospital after being found unresponsive at home. She was noted to have acute kidney injury (serum creatinine 789 $\mu\text{mol/l}$) and a severe metabolic acidosis (pH 7.09; HCO_3^- 2 mmol/l ; pCO_2 5 mm Hg). She had no relevant past medical history and had a previously recorded serum creatinine of 51 $\mu\text{mol/l}$. As the cause of her acute kidney injury was unknown, a renal biopsy was performed on day 7 of her admission, which demonstrated acute oxalate nephropathy with significant deposition of CaOx in the renal parenchyma. Further investigation demonstrated a toxic level of serum

ethylene glycol (8.8 mmol/l). She required 14 days of intermittent hemodialysis before renal recovery, and her serum creatinine remained elevated (102 $\mu\text{mol/l}$) 3 months after discharge.

To investigate the relationship between oxidative stress and the recruitment of inflammatory cells following acute oxalate nephropathy, excess fresh renal cortical tissue from the biopsy was obtained with informed consent and institutional ethics approval (Royal Brisbane and Women's Hospital Human Research Ethics Committee 2006/072).

Flow-cytometric analysis was performed after digesting the biopsy tissue with 1 mg/ml collagenase P (Roche, Mannheim, Germany) in the presence of 20 $\mu\text{g/ml}$ DNase I (Roche) (250- μl volume) for 15 minutes and then further digesting with a mixture of 10 $\mu\text{g/ml}$ trypsin and 4 $\mu\text{g/ml}$ ethylenediamine tetraacetic acid (Life Technologies, Grand Island, NY) (500- μl volume) for 10 minutes (Figure 1). Single-cell suspensions were initially stained with LIVE/DEAD Fixable Near-IR Dead Cell Stain Kit (Life Technologies) to exclude nonviable cells. Cells were then incubated with Human TruStain FcX Blocking Solution (Biolegend, San Diego, CA) at room temperature for 5 to 10 minutes and then stained on ice for 30 minutes with mouse antihuman CD45, CD14, CD3 antibodies in cold fluorescence-activated cell-sorting buffer (0.5% bovine serum albumin [Sigma, St. Louis, MO] and 0.02% sodium azide [Sigma] in phosphate-buffered saline solution). Cell acquisition was performed on an LSR Fortessa (BD Biosciences, Sparks, MD) and data analyzed with FlowJo software (TreeStar, Ashland, OR).

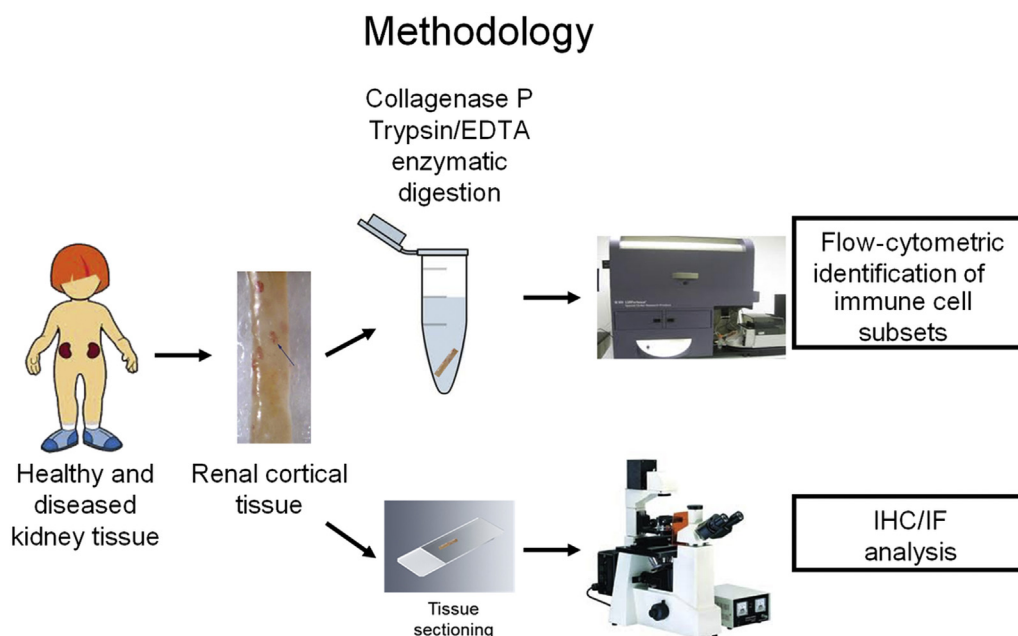


Figure 1. Study methodology. EDTA, ethylenediaminetetraacetic acid; IF, immunofluorescence; IHC, immunohistochemistry.

Immunofluorescence staining was performed on frozen 7- μm tissue sections that were fixed with 25% ethanol:75% acetone at room temperature for 5 minutes, followed by a protein block with Background Sniper Blocking Reagent for 30 minutes (Biocare Medical, Concord, CA) (Figure 1). Sections were subsequently probed with anti-CD3 (rabbit polyclonal IgG; Agilent Technologies, Santa Clara, CA) and anti-CD68 (monoclonal mouse IgG3; Clone PG-M1; Agilent) at room temperature for 1 hour. Fluorescent detection was obtained by secondary incubation with AlexaFluor-488 antimouse IgG and AlexaFluor-647 antirabbit IgG (Life Technologies) at room temperature for 30 minutes. Nuclei were stained with 4',6-diamidino-2-phenylindole (DAPI; Life Technologies). Slides were coverslipped in fluorescence mounting medium (Agilent Technologies). A Zeiss 780 NLO confocal microscope (Carl Zeiss, Hamburg, Germany) was used for fluorescence microscopy. Image acquisition and analysis were performed using ZEN software (Carl Zeiss).

Immunohistochemical staining was also performed on frozen 7- μm tissue sections that were fixed with 25% ethanol:75% acetone at room temperature for 5 minutes (Figure 1). Endogenous peroxidase activity was blocked with 1% H_2O_2 for 10 minutes, followed by a protein block with 2% bovine serum albumin in Odyssey Blocking Buffer (Li-Cor, Lincoln, NE). Sections were probed with anti-4-hydroxynonenal (4-HNE) (goat polyclonal IgG; Abcam, Cambridge, MA) and anti-phosphorylated mixed lineage domain-like protein (p-MLKL) (monoclonal rabbit IgG; Abcam) at room temperature for 1 hour. Tissue sections were washed, and a goat or rabbit horseradish peroxidase polymer system (Biocare Medical) was applied according to the manufacturer's instructions. Peroxidase activity was developed with DAB substrate for 5 minutes. Sections were lightly counterstained with hematoxylin and mounted using DPX mounting medium. All analyses were compared to healthy renal cortical tissue as a control.

Polarized light microscopy confirmed the presence of CaOx deposits within the renal interstitium (Figure 2a) of our patient. There was a significant increase in 4-HNE renal expression compared to the healthy control (44.40 vs. 3.18 positive pixel intensity/ μm^2 ; $P < 0.001$) with foci of higher 4-HNE renal expression co-localizing with the CaOx crystals (Figure 2b). Evidence from animal studies suggests that CaOx induces lipid peroxidation of the renal tubular membranes, which increases oxygen reactive species and consequently oxidative stress.^{3,5,6} 4-HNE represents one of the most bioactive products of lipid

peroxidation, and plays an important role mediating numerous signaling pathways including the inflammatory response.⁷ The increased renal expression of 4-HNE in our patient is similar to that seen in these previous animal and cell line studies, and provides support for the same pathogenic mechanism occurring in humans.

In addition to inducing oxidative stress, CaOx crystal deposition has also been shown to cause direct cytotoxic effects on renal tubular cells, and this may lead to necrotic cell death.^{8,9} The term "necroptosis" has recently been used to describe this regulated form of cell necrosis triggered by crystal deposition.¹⁰ The signal transduction pathway of necroptotic cell death is mediated by ligation of tumor necrosis factor alpha to its receptor. This ultimately results in the phosphorylation of MLKL, which, once phosphorylated, translocates to the plasma membrane where it disrupts plasma membrane integrity.^{8,10,11} The significant tubular positivity for p-MLKL found in our patient compared to the healthy control (Figure 2c) provides corroborating evidence for the role of necroptosis-mediated cell death from acute oxalate nephropathy. Furthermore, the strong tubular positivity of p-MLKL in our patient was associated with the increased expression of 4-HNE. This supports the recently emerging concept that necroptosis may trigger further inflammation, whereas reactive oxygen species may act as critical regulators of necroptotic signaling.^{10,11}

Immunofluorescence demonstrated an increased infiltration of macrophages (CD68) and T cells (CD3) with foci of activity around calcium oxalate crystals (Figure 2d). There was a marked increase in leukocytes (26% vs. 3% CD45^+ cells) by flow cytometry in our patient compared to the healthy control (Figure 2e and f). These leukocytes were predominantly mononuclear cells (85% of leukocytes), of which 47% were T cells (CD3) and 29% were monocytes (CD14). Previous animal studies have shown that CaOx within the renal interstitium activates the immune system via macrophages and monocytes.^{1,12} Similarly, the renal parenchyma of our patient was also infiltrated with monocytes, macrophages, and T cells (CD3), with a more intense infiltration of inflammatory cells around CaOx crystals. Our results support previous findings suggesting that CaOx-generated oxidative stress recruits effector cells via monocytes and macrophages,^{4,5,11} and suggests that the immune responses observed in animal and cell line studies may also occur in humans.

Although our study was able to describe an association among renal CaOx deposition, oxidative stress,

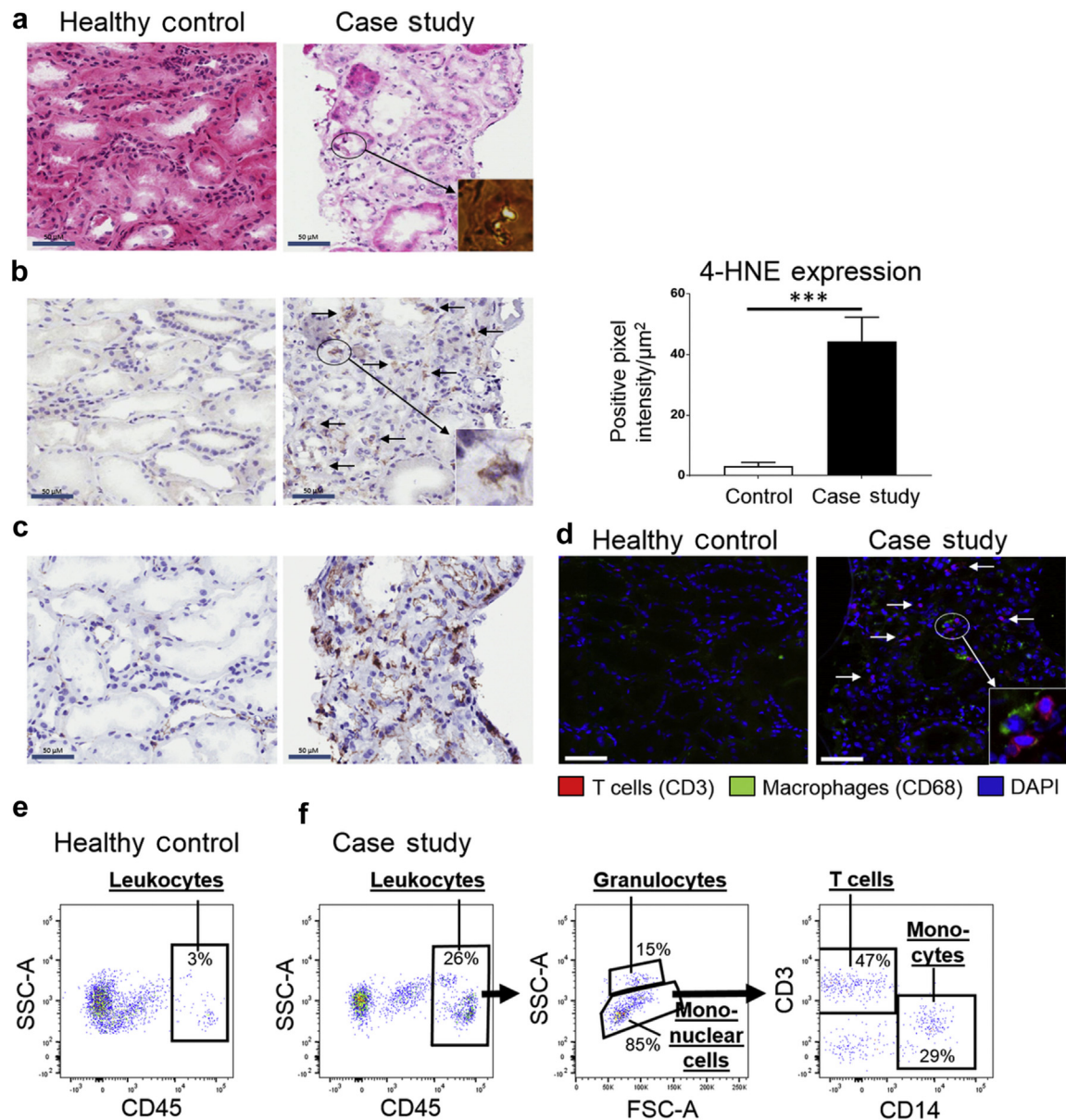


Figure 2. (a) Hematoxylin (purple) and eosin (pink) staining of frozen kidney sections from healthy control (left) and case study (right) tissue under light microscopy and with polarization (right, inset) to visualize oxalate crystals. (b) Immunohistological labeling of healthy control (left) and case study (right) frozen tissue stained for 4-hydroxynonenal (4-HNE). Bars=50 μm . Quantitative analysis (positive pixel intensity/ μm^2 area) of 4-HNE staining. Results represent mean \pm SD of values from 3 randomly selected areas for each tissue sample. *** $P < 0.001$, unpaired t test. (c) Immunohistological labeling of healthy control (left) and case study (right) frozen tissue stained for phosphorylated mixed lineage domain-like protein (p-MLKL). Bars=50 μm . (d) Immunofluorescent labeling of healthy control (left) and case study (right) frozen tissue stained for CD3 (red) and CD68 (green). Bars=50 μm . (e, f) Multicolor flow-cytometric identification of immune cells (gated on live, singlet cells) in healthy control (e) and case study (f) kidney tissue. DAPI, 4',6-diamidino-2-phenylindole.

and inflammation, a causal relationship cannot be proved. For obvious ethical reasons, we were limited to a single time-point collection of kidney tissue, and we were not able to describe the sequence of immunological responses to renal CaOx deposition. Of note, our patient did not have pre-existing chronic kidney disease, and our findings are therefore likely to represent only the pathological response to acute CaOx deposition.

In summary, we describe the presence of increased renal oxidative stress, evidence of activated necroptotic pathways, and renal inflammation in a patient with acute oxalate nephropathy secondary to ethylene glycol intoxication. Our findings are the first to translate previous animal and cell line studies^{2,3,5,6} into humans, and suggest a shared pathogenic mechanism of renal CaOx deposition, increased oxidative stress, inflammation, and necroptosis.

Gregory J. Wilson^{1,2}, Pedro H.F. Gois^{1,2},
Alice Zhang^{1,2,3}, Xiangju Wang^{1,3}, Becker
M.P. Law^{1,3,4}, Andrew J. Kassianos^{1,2,3,4} and
Helen G. Healy^{1,2,3}

¹Department of Renal Medicine, Royal Brisbane and Women's Hospital, Brisbane, Queensland, Australia; ²School of Clinical Medicine, Royal Brisbane Clinical Unit, Faculty of Medicine, University of Queensland, Brisbane, Queensland, Australia; ³Conjoint Kidney Research Laboratory, Pathology Queensland, Brisbane, Queensland, Australia; and ⁴Institute of Health and Biomedical Innovation/School of Biomedical Sciences, Queensland University of Technology, Brisbane, Queensland, Australia

Corresponding author: Gregory J. Wilson, Department of Renal Medicine, Royal Brisbane and Women's Hospital, Herston, Queensland 4029, Australia. E-mail: gregory.wilson@health.qld.gov.au

DISCLOSURE

All the authors declared no competing interests.

ACKNOWLEDGMENTS

This work was funded by Pathology Queensland, the Kidney Research Foundation and a National Health and Medical Research Council (NHMRC) Project Grant (GNT1099222).

REFERENCES

1. Khan SR. Crystal-induced inflammation of the kidneys: results from human studies, animal models, and tissue-culture studies. *J Clin Exp Nephrol*. 2004;8:75–88.
2. Shimizu MHM, Gois PHF, Volpini RA, et al. N-acetylcysteine protects against star fruit-induced acute kidney injury. *Ren Fail*. 2017;39:193–202.
3. Thamilselvan S, Hackett RL, Khan SR. Lipid peroxidation in ethylene glycol induced hyperoxaluria and calcium oxalate nephrolithiasis. *J Urol*. 1997;157:1059–1063.
4. Kusmartsev S, Dominguez-Gutierrez PR, Canales BK, et al. Calcium oxalate stone fragment and crystal phagocytosis by human macrophages. *J Urol*. 2016;195:1143–1151.
5. Umekawa T, Chegini N, Khan SR. Oxalate ions and calcium oxalate crystals stimulate MCP-1 expression by renal epithelial cells. *Kidney Int*. 2002;61:105–112.
6. Sharma M, Kaur T, Singla SK. Role of mitochondria and NADPH oxidase derived reactive oxygen species in hyperoxaluria induced nephrolithiasis: therapeutic intervention with combinatorial therapy of N-acetyl cysteine and Apocynin. *Mitochondrion*. 2016;27:15–24.
7. Zhong H, Yin H. Role of lipid peroxidation derived 4-hydroxynonenal (4-HNE) in cancer: focusing on mitochondria. *Redox Biol*. 2015;4:193–199.
8. Mulay SR, Desai J, Kumar SV, et al. Cytotoxicity of crystals involves RIPK3-MLKL-mediated necroptosis. *Nat Commun*. 2016;7:10274.
9. Sun X-Y, Gan Q-Z, Ouyang J-M. Calcium oxalate toxicity in renal epithelial cells: the mediation of crystal size on cell death mode. *Cell Death Discov*. 2015;1:15055.
10. Fulda S. Regulation of necroptosis signaling and cell death by reactive oxygen species. *Biol Chem*. 2016;397:657–660.
11. Berghe TV, Linkermann A, Jouan-Lanhouet S, et al. Regulated necrosis: the expanding network of non-apoptotic cell death pathways. *Nat Rev Mol Cell Biol*. 2014;15:135–147.
12. de Water R, Noordermeer C, van der Kwast TH, et al. Calcium oxalate nephrolithiasis: effect of renal crystal deposition on the cellular composition of the renal interstitium. *Am J Kidney Dis*. 1999;33:761–771.

Received 11 March 2018; revised 3 May 2018; accepted 7 May 2018; published online 11 May 2018

Kidney Int Rep (2018) 3, 1217–1221; <https://doi.org/10.1016/j.ekir.2018.05.005>

© 2018 International Society of Nephrology. Published by Elsevier Inc. This is an open access article under the CC BY-NC-ND license (<http://creativecommons.org/licenses/by-nc-nd/4.0/>).